Journal of Kerbala University , Vol. 6 No.3 Scientific. 2008

Model optimization of SOA used in ultra-high bit rate OTDM demultiplexer

أنموذج مثالي للمضخمات البصرية المستخدمة في أنظمة الاتصالات الضوئيه عالية السرعة

Prof. Dr. Raad S. Fyath Dr.Ibrahim A.Murdas

Abstract

The ultrafast femtosecond gain and phase dynamics of semiconductor optical amplifier (SOA) are investigated in this work. Acomprehensive model is developed which takes in to account interband transition, intraband transition SHB, CH, TPA, polarization state of control pulse and data . the model is used to extract the femotosecond switching dynamics of the SOA under different operating condition such as injection current ,control pulse power ,control pulse polarization ,SOA length and TPA.

الملخص

في هذا العمل تم دراسة داينميكا الطور و الربح للمضخمات الشبه موصله في أزمان سريعة جدا .ثم تم تطوير أنموذج شامل يأخذ بنظر الاعتبار كل من الانتقالات SHB,CH,TPA(interband, and intraband) وكذلك وحالة الاستقطاب لنبضة السيطرة و البيانات . الأنموذج استخدم لاستخراج داينميكا المفاتيح في femtosecond تحت شروط تشغيل مختلفة مثل حقن التيار و قدرة نبضة السيطرة واستقطاب نبضة السيطرة و طول المضخمات وكذالك TPA.

I. INTRODUCTION

Semiconductor optical amplifiers (SOA's) are important components for optical networks. On the other hand, potential use of SOAs' nonlinearities for all-optical signal processing has led to research in various application fields [1,2].all-optical switching is one of the key components in all-optical signal processing for ultra high speed applications[3]. all-optical demultiplexer for TDM data signals with a line bit rate of up to 160 Gb/s.

has been demonstrated [4, 5]. The potential of SOA's has led to the development of various theoretical models, see, [6,7]. A quite successful description of the SOA gain dynamics that includes the ultrafast gain dynamics and its saturation has been presented by Mecozzi and Mørk in [8] and [9]. In this respect, the all-optical switching has been one of the most investigated components in all-optical time-division multiplexing (OTDM) communication networks. An interesting all-optical switch that allows ultrafast operation consists of a semiconductor optical amplifier (SOA) in an interferometric structure. All-optical switches based on nonlinearities in SOAs are considered important building blocks in optical telecommunication systems [10,11]. Optical switching in the picoseconds regime has been shown using a Varity of configuration such as the symmetric mach-zahender interferometer (SMZ) the ultrafast nonlinear interferometer (UNI), Terahertz optical asymmetric demultiplexer(TOAD). Starting from SOA- based nonlinear interferometric structures and using optical nonlinearities in semiconductors materials, various approaches have been proposed and used for all-optical signal processing. All – optical interferometric switches based on SOA have been successfully applied in a number of high bit rate time division demultiplexing experiments [12]. The SOA dynamics model takes into account the carrier dynamics on femtosecond time scale driving by two-photon absorption (TPA) and free carrier absorption (FCA). The model is suitable for investigating and optimizing the performance of an SOA in a system environment.

II. Modeling

A. Mechanism behind SOA gain dynamics.

The gain of the SOA results form transitions between the conduction and valence bands. These transitions depend on the carrier density and on the carrier distribution in both bands. In order to distinguish the different physical processing, it is useful to consider interband and intraband processing separately.

B. Rate equation

We present briefly the rate equations that describe the carrier dynamics in an active semiconductor material. A derivation of the rate equations based on the concepts interband and intraband transitions on SOA. The interband processes change the carrier density (N) but don't affect the carrier distribution. The carrier density rate equation is given by [13].

$$\frac{\partial N}{\partial t} = \frac{J_e}{ed} - R(N) \qquad \text{---- (1)}$$

Where Je= Current density. e = Electron charge. d= Active layer thickness. R (N) = Carrier loss caused by various radiative and non-radiative recombination processes. The parameter R (N) can be separated into three component , spontaneous emission rate R_{spon}, stimulated emission rate R_{stim} , and amplified spontaneous emission rate R_{ASE} [13].

$$R(N) = R_{spon} + R_{stim} + R_{ASE} \qquad \text{---(2)}$$

For the spontaneous recombination rate [8]

$$R_{spon} = A_{nonrad} N + B_{spon} N^2 + C_{Auger} N^3 \qquad \text{---- (3)}$$

The coefficients in equation (3) denote non- radiative processes, spontaneous emission, and Auger recombination, respectively. The stimulated recombination rate describes the impact of stimulated emission and absorption. It can be written as

$$R_{stim} = v_g g(z,t) S(z,t) \qquad \text{---(4)}$$

Where $g(z,t)$ = Group velocity, z = Longitudinal axis of the SOA, $S(z,t)$ = Intensity of the electric field. v_g = Gain coefficient of SOA.

The parameter R_{ASE} accounts for the carrier recombination, stimulated by the spontaneously emitted photons, which are not included in the signal photon density S(z,t).

The phase dynamics of active semiconductor materials are usually described using the α -factor. The α - factor is defined as the ratio of the changes of the real to the imaginary part of the material refractive index and can be expressed as [14]

$$\alpha = -\frac{4\pi}{\lambda} \frac{\frac{\partial n_{ref}}{\partial N}}{\frac{\partial g_N}{\partial N}} \qquad \text{----(5)}$$

Where λ= Wavelength in vacuum. n_{ref} =Refractive index. g_N = Gain coefficient that depends on carrier density. to calculate the field phase at the SOA output, one needs to know the field phase at a Φ_{inp} reference carrier density (N) [14].

$$\Phi(N) = \Phi_{inp} - \frac{1}{2}\alpha \Delta g_N L \qquad \text{----(6)}$$

Where L is the length of active medium. This equation gives the phase shift at the SOA output with a gain variation (Δg_N).

Due to the differential form of the definition of the α factors, the phase shift at the output Φ_{out} is obtained by summing up every involved component

$$\Phi_{out} = \Phi_{inp} - \frac{1}{2} L(\alpha \Delta g_N + \alpha_{CH} g_{CH} + \alpha_{SHB} g_{SHB} + \alpha_2 g_{TPA}) \qquad \text{----(7)}$$

where α_{CH} = Carrier heating linewidth enhancement factor. g_{CH} = Temperature – dependent gain change. α_{SHB} = Spectral hole burning linewidth enhancement factor. g_{SHB} = gain change induced by spectral hole burning. α_2 = Two-photon absorption linewidth enhancement factor. g_{TPA} = Gain change due to two photon absorption. Φ_{inp} = phase at reference carrier density.

When the input pulse width is shorter than few hundreds of femtoseconds and with energies larger than some hundreds of femtojoules the contribution of carrier heating and spectral hole burning can be neglected [15]. Equation 7 becomes

$$\Phi_{out} = \Phi_{inp} - \frac{1}{2} L(\alpha \Delta g_N + \alpha_2 g_{TPA}) \qquad \text{---(8)}$$

The phase change of the input signal at the SOA output is

$$\Delta\Phi = \Phi_{out} - \Phi_{inp} = -\frac{1}{2} L(\alpha \Delta g_N + \alpha_2 g_{TPA}) \qquad \text{---(9)}$$

The parameter g_{TPA} is given by

$$g_{TPA} = \beta_2 \Gamma_2 S(z,t) \qquad \text{--- (10)}$$

Where β_2 =TPA coefficient. Γ_2 = Confinement factor of the TPA.

Substitution equation (10) into (9) yields

$$\Delta\Phi = -\frac{1}{2}(L\alpha \Delta g_N + L\alpha_2 \Gamma_2 \beta_2 S(z,t)) \qquad \text{--(11)}$$

The polarization- dependent gain saturation is taken into account by assuming that the polarized optical field can be decomposed into transverse electronic (TE) and transverse magnetic (TM) components that propagate "independently" through the SOA; although they have indirect interaction with each other via the gain saturation account for different TE and TM gains by assuming that these polarization couple to different hole reservoirs. The propagation of the electromagnetic field inside the amplifier is governed by the wave equation

$$\nabla^2 E - \frac{\varepsilon}{c^2}\frac{\partial^2 E}{\partial^2 t^2} = 0 \qquad \text{---(12)}$$

where: c = Velocity of light in vacuum. ε =Dielectric constant of the medium and it is given by [16]

$$\varepsilon = n_b^{\,2} + \chi \qquad \text{---(13)}$$

Here n_b is the background refractive index. The χ represents the contribution of the charge carriers inside the active region of the amplifier and is a function of carrier density N [16].

$$\chi(N) = -\frac{n'c}{\omega_0}(\alpha + j)a_N(N - N_0) \qquad \text{---(14)}$$

where n' = Effective mode index , a_N= Differential gain coefficient N_0 =Carrier density at transparency, α = Linewidth enhancement factor. ω_0 = $2\pi/\lambda$= Optical radian frequency j =. The gain coefficient depends on carrier density (N).

$\sqrt{-1}$

$$g_N = a_N(N - N_0) \qquad \text{--(15)}$$

Substituting equation 15 into 14 yields

$$\chi(N) = \frac{-n'c}{\omega_0}(\alpha + j)g_N \qquad \text{---(16)}$$

Assuming that the input light is linearly polarized and remains linearly polarized during propagation, the electric field inside the amplifier can be written as

$$E(x, y, z, t) = \hat{x}\frac{1}{2}\left\{F(x, y)A(z, t)\exp^{[j(k_0 z - \omega_0 t)]} + c.c\right\} \qquad \text{-- (17)}$$

$\hat{x}$

where = Polarization unit vector, F(x, y)= Waveguide- mode distribution , A (z, t) = Slowly- varying envelope associated with optical pulse, .

The complex field amplitude can be related to the intensity $S(z,t)$ and the phase through the well known relationship$\Phi(z,t)$

$$A(z,t) = \sqrt{S(z,t)}\exp^{j\Phi(z,t)} \qquad \text{-- (18)}$$

Substituting equation 17 into equation 12 neglecting the second derivative of $A(z,t)$ with respect to z and t, and integrating over the transverse dimensions, and also take the internal losses into account yields

$$\frac{\partial A}{\partial Z} + \frac{1}{v_g}\frac{\partial A}{\partial t} = \frac{j\omega_0\Gamma}{2n'c}\chi(N)A(z,t) - \frac{1}{2}\alpha_{in}A(z,t) \qquad \text{--- (19)}$$

α_{in}

where = Internal losses. Substituting equations 16 into equations 19 yields[6] .

$$\frac{\partial A}{\partial Z} + \frac{1}{v_g}\frac{\partial A}{\partial t} = \frac{1}{2}\Gamma(1 + j\alpha)g_N A(z,t) - \frac{1}{2}\alpha_{in}A(z,t) \qquad \text{---(20)}$$

The analysis is taken further by adding two extra effects TPA and FCA to the pulse propagation equation (equation 20). The TPA gain coefficient is related to the phase of the (TPA) ϕ_{TPA} by

$$\phi_{TPA} = -\frac{1}{2}\alpha_2 g_{TPA} \qquad \text{--- (21)}$$

The FCA gain reduction effect in the conduction and valence bands are [14]

$$g_{ch} = \beta_v n_h(z,t) \quad \text{--- (22a)}$$

$$g_{ch} = \beta_c n_e(z,t) \quad \text{-- (22b)}$$

where α_2 = Linewidth enhancement factor of TPA. β_v = FCA coefficient in valence bands. = FCA coefficient in conduction bands. β_c : Electrons density in the conduction bands $n_e(z,t)$ $n_h(z,t)$ Holes density in the valence bands.

The propagation equation 20 can be now modified to include the effects of the ultrafast dynamics and carrier heating. Inserting equations 10, 21 and 22a, 22 b into equation 20 yields

$$\frac{\partial A}{\partial Z} + \frac{1}{v_g}\frac{\partial A}{\partial t} = \begin{bmatrix} \frac{1}{2}\Gamma(1-j\alpha)g_N - \frac{1}{2}\alpha_{in} - \frac{1}{2}\Gamma_2\beta_2(1+j\alpha_2)S(z,t) - \frac{1}{2}\Gamma\beta_c n_e(z,t) - \\ \frac{1}{2}\Gamma\beta_v n_h(z,t) \end{bmatrix} A(z,t) \quad \text{---(23)}$$

To take the effect of polarization on SOA dynamics, the incoming polarized electric field is decomposed in a component parallel to the layers in the waveguide (x component, TE-mode) and a perpendicular component (y component, TM mode). These two polarization directions are along the principle axes ($\hat{x},\hat{y}$) that diagonals the wave propagation in the SOA. The electric field components are given by

$$E^{TE/TM}(z,t) = \left\{ [A^{TE}(z,t)\hat{x} + A^{TM}(z,t)\hat{y}] \exp^{[j(k_0 z - \omega_0 t)]} + c.c \right\} \quad \text{----(24)}$$

The propagation equation for TE and TM modes becomes, respectively

$$\frac{\partial A^{TE}}{\partial Z} + \frac{1}{v_g}\frac{\partial A^{TE}}{\partial t} = \begin{bmatrix} \frac{1}{2}\Gamma^{TE}(1+j\alpha)g^{TE}{}_N - \frac{1}{2}\alpha_{in} - \frac{1}{2}\Gamma_2\beta_2(1+j\alpha_2)[S^{TE}(z,t) + \\ S^{TM}(z,t)] - \frac{1}{2}\Gamma\beta_c n_e(z,t) - \frac{1}{2}\Gamma\beta_v n_x(z,t) \end{bmatrix} A^{TE}(z,t) \quad \text{--(25)}$$

Where the super script TE(TM) refers to TE(TM) polarization state. The rate equation of electrons is not effect by the TE and TM components

$$\frac{\partial n_e}{\partial t} = \frac{n_e(z,t) - n'_e(z,t)}{\tau_{1c}} - v_g g(z,t)S(z,t) - n_e(z,t)\beta_c v_g S(z,t) \quad \text{--- (26)}$$

Where τ_{1c}= Carrier-carrier scattering times. $n'_e(z,t)$ Quasi-equilibrium values of the electron carrier density. The rate equation of the holes is affected by the polarization- dependent model because holes have two reservoirs identified with index x and y. Holes identified with (x) couple with electrons through TE polarized light. Similarly, holes identified with (y) couple with electrons trough TM polarized light.

$$\frac{\partial n_h}{\partial t} = -\frac{n_h(z,t) - n'_h(z,t)}{\tau_{1v}} - v_g g(z,t)S(z,t) - n_h(z,t)\beta v_g S(z,t) \quad \text{--- (27)}$$

Therefore equation (27) becomes [17]

$$\frac{\partial n_x}{\partial t} = -\frac{n_x(z,t) - n'_x(z,t)}{\tau_{1v}} - v_g g^{TE}(z,t) S^{TE}(z,t) - n_x(z,t)\beta_v v_g [S^{TE}(z,t) + S^{TM}(z,t)] \quad \text{-- (28)}$$

$$\frac{\partial n_y}{\partial t} = -\frac{n_y(z,t) - n'_y(z,t)}{\tau_{1v}} - v_g g^{TM}(z,t) S^{TM}(z,t) - n_y(z,t)\beta_v v_g [S^{TE}(z,t) + S^{TM}(z,t)] \quad \text{-- (29)}$$

The equation for the total electron-hole pair density $N(z,t)$ can be expressed as

$$\frac{\partial N(z,t)}{\partial t} = \frac{I}{eV} - \frac{N}{\tau_s} - v_g [g(z,t) S(z,t)] + v_g \beta_2 S^2(z,t) \quad \text{--- (30)}$$

where I= Injection current to the SOA. V= Active volume of the SOA. τ_S = Electron – hole pair lifetime.

For the polarization dependent model the electron-hole pair density N (z, t) becomes

$$\frac{\partial N(z,t)}{\partial t} = \frac{I}{eV} - \frac{N}{\tau_s} - v_g [g^{TE}(z,t) S^{TE}(z,t) + g^{TM}(z,t) S^{TM}(z,t)] + v_g \beta_2 [S^{TE}(z,t) + S^{TM}(z,t)]^2 \quad \text{--- (31)}$$

The energy densities satisfy [17]

$$\frac{\partial U_v(z,t)}{\partial t} = [\beta_v \hbar \omega_0 n_h(z,t) - E_v g(z,t)] S^{TE}(z,t) v_g - \beta_{2v} v_g E_{2v} S^2(z,t) - \frac{U_v(z,t) - U'(z,t)}{\tau_{hv}} \quad \text{--(32)}$$

where E_v and E_{2v} = Optical transition energies(conduction band) τ_{hv} = Carrier – phonon interaction time $U'_v(z,t)$ = Quasi-equilibrium energy.

The energy density in polarization dependent model is [17]

$$\frac{\partial U_c(z,t)}{\partial t} = \beta_c \hbar \omega_0 n_e(z,t) v_g [S^{TE}(z,t) + S^{TM}(z,t)] - E_c v_g [g^{TE}(z,t) S^{TE}(z,t) + g^{TM}(z,t) S^{TM}(z,t)] + E_{2c} v_g \beta_2 [S^{TE}(z,t) + S^{TM}(z,t)]^2 - \frac{U_c(z,t) - U'_c(z,t)}{\tau_{hc}} \quad \text{-(33a)}$$

$$\frac{\partial U_v(z,t)}{\partial t} = \beta_v \hbar\omega_0 v_g [n_x(z,t) + n_y(z,t)][S^{TE}(z,t) + S^{TM}(z,t)] - E_v v_g [g^{TE}(z,t)S^{TE}(z,t) + g^{TM}(z,t)S^{TM}(z,t)] + E_{2v} v_g \beta_2 [S^{TE}(z,t) + S^{TM}(z,t)]^2 - \frac{U_v(z,t) - U'_v(z,t)}{\tau_{hv}} \quad \text{-- (33b)}$$

Where $U_C(z,t)$ = Energy density in the conduction band. and = Optical transition energy (valence band)

III. Gain and Phase Dynamics under various operation conditions

The set of equations 24 - 33 presented in the previous sections is solved numerically using standards methods as shown in Figure 1 to access the dynamics of the SOA in the presence of both data and control pulses as shown in Figure 2. The values of the parameters used in the simulations are listed in Table (1) and they are related to multi quantum well (MQW) SOA. These parameters setting leads to results that are in good agreement with measured gains amplification and net phase between two components TE and TM , as presented in .

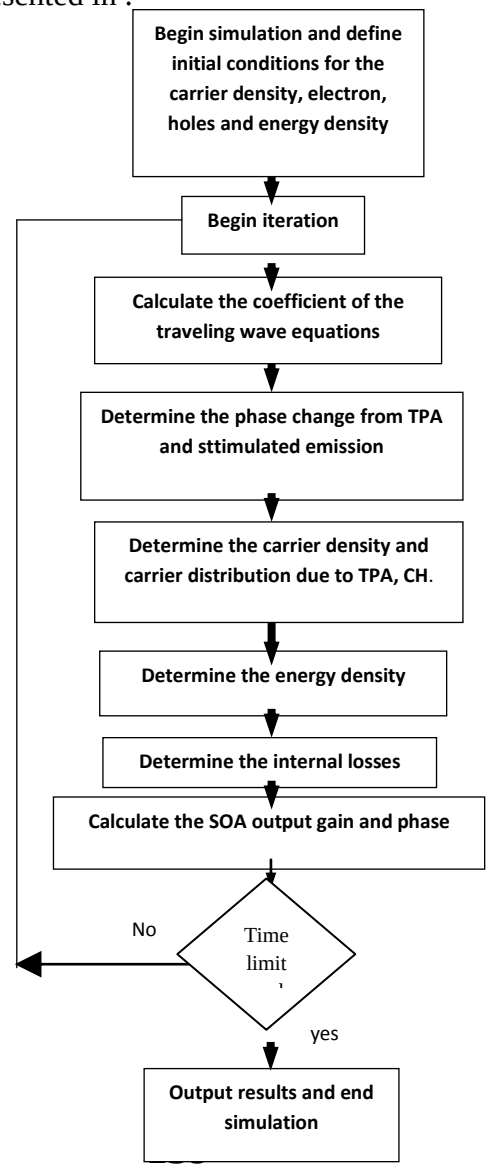

Table (1.1) Parameters definitions and values for MQW-SOA

Parameter Unit	*Symbol*	*Value*
Active Volume	V=L*w*d	750*2*0.1 μm
Wave length of control pulse	λ_c	1520 nm
Pulse width	t_p	200 fs
Energy of control pulse	E_c	3.2 pJ
Energy of data pulse with TE polarization state	E_d	0.32 pJ
Injection current	I	0 or 180 mA
Carrier life time	τ_c	1.3 nsec
Line width enhancement factor	α	1.2
Line width enhancement factor of TPA	α_2	-1.5
Initial carrier density	N_0	4.8e15
Confinement factor	Γ_{TE} Γ_{TM} Γ_{TPA}	0.032 0.021 0.09
TPA coefficient	β_{TPA}	$9*10^{-7}$ μm^2

A. Effect of control pulse energy

To check the accuracy of the developed SOA dynamics model, a comparison is made between a published experimental data [18] and our theoretical predications. The results depicted in Figure 2 which illustrates the variation of data (prope) amplitude with control pulse energy for two control polarization states TE and TM. The parameters values used in the simulation are identical to those given in Ref. [18]. A 0.8fJ, 200 fs TE polarized prope pulse is assumed. The marks in the figure denote the experimental data of Ref. [18] while the solid lines denote simulation results predicted by our model. Figure 2 reveals that theoretical predications are in good agreement with the experimental data. Investigation Figure 2 highlights the fact that prope data experience less gain in the presence of control pulse. This is because the gain temporally decreases after the simulated emission induced by the strong control pulses. It follows from Figure 2 that TE amplification is the smallest for TE control, being reduced by about 18 dB when the control pulse energy is 0.8 pJ. This amplification is about 1.5 dB larger if the control pulse is TM polarized. We Carry the calculation further to investigate the dependence of phase shift ($\Delta\Phi$) on the injection current for different

values of control pulse energy. The results are illustrated in Figure 3 for control probe delay ($\Delta\tau$ =2.5 ps) .Note that the phase shift depends on the input control pulse energy; high input control pulse yields high phase shift at certain injection current.

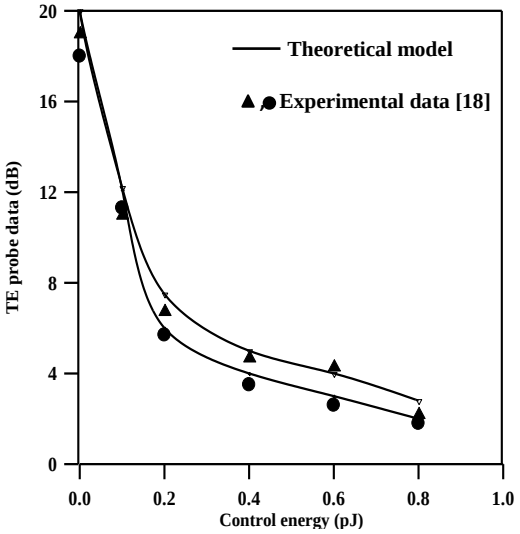

Figure 2 Simulation of the amplification of a 0.8 fJ, 200 fs TE polarized probe pulse as a function of the control pulse energy.

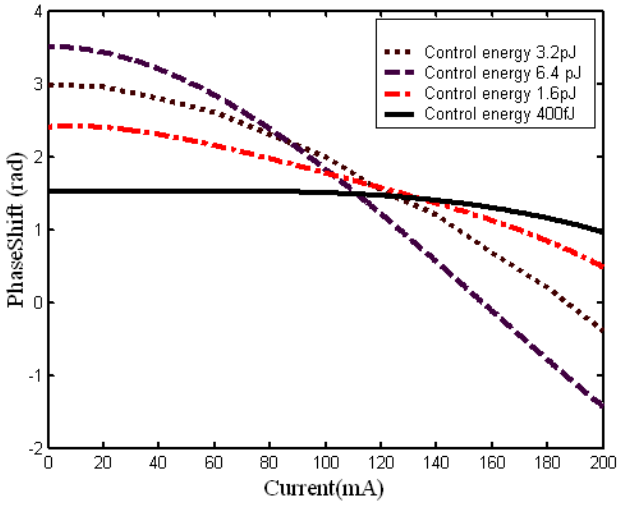

Figure 3 nonlinear phase shift as a function of the injection current for various control energy at control prob delay 2.5 ps.

B. Effect of TPA on gain dynamics

Figures 4a and b shows the gain compression induced by control pulses in the presence (absence) of TPA. Note that the presence of TPA increase the gain compression and shows a fast recovery. For example at 2.5 ps , the gain compression is 0.11 μm^{-1} (0.06 μm^{-1}) in the presence (absence)of TPA. This result can be explained as follows the observed long recovery time in absence TPA referred to long relaxation time compared to TPA relaxation time where the TPA contribution is one order of magnitude smaller than the recovery of CH and SHB. The compression in presence TPA is larger because this compression related to TPA reduction through the absorption of photons.

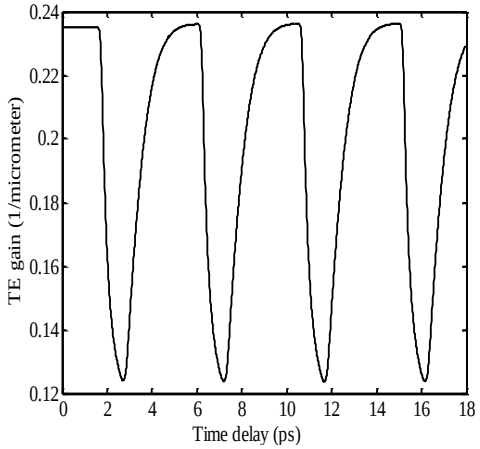

(a)

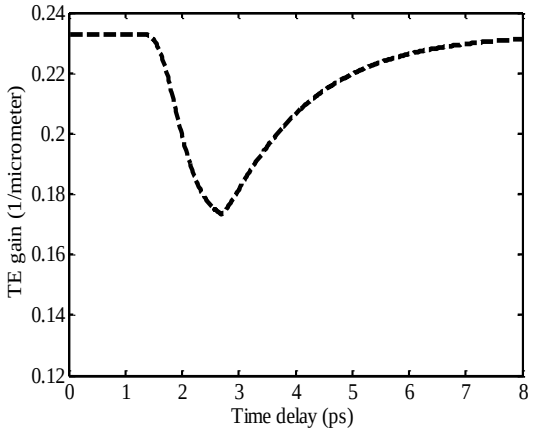

(b)

Figure 4a,b Time variation of gain coefficient TE polarization component a) with TPA effect b) Without TPA effect

C. Effect of control signal polarization

Figures 5 a and b show, respectively, the time delay dependence of TE gain for TE and TM control polarization, respectively. Figures 5 a and b indicate clearly that the first TE gain minimum occurs at (t=2.5ps) which corresponds to the middle of the 250μm SOA cavity. The results show that the decrease in the TE data gain is higher if the control is also TE polarized as a compared with the case if the control signal is TM polarized. Note that at (t =2.5ps), the gain coefficient is reduced by $0.11\mu m^{-1}$ ($0.08\ \mu m^{-1}$) for TE (TM) control pulses. It can also be noted from Figure 5 that an initial gain recovery at a 0.8ps timescale appears, then followed by a slow recovery time, which is associated with the interband effects determined by the electron and hole recombination times (1.3 ns)

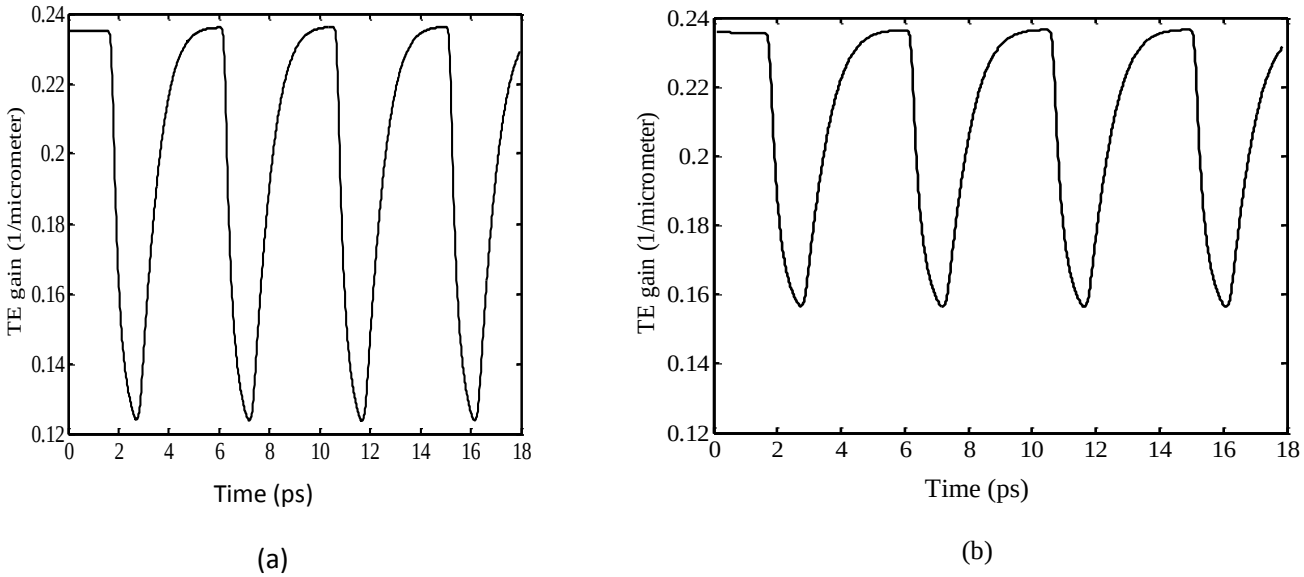

Figure 5a,b Time variation of gain coefficient when the control pulse is a) TE and b) TM polarization state. The pulse energy for control and data is 1.7pJ and, 0.8fJ, respectively.

Because the gain temporarily decreases after the stimulated emission induced by the strong control pulses, the probe pulse that follows will experience less amplification than when there is no control pulse present.

D. Effect of injection current

Figure 6 shows the dependence of the nonlinear phase shift on the injection current as function of the control -data delay (Δt). The doted line in the figure 6 shows the nonlinear phase shift for 0mA injection current, while the solid line shows the same results but now for an injection current 180 mA.

Investigation this figure reveals the following

i. The maximum values of the nonlinear phase shift occur at = 2.5ps.

ii. The recovery time of the nonlinear phase shift is approximately (2ps).This is very important in ultrafast switching window. The recovery time decreases with injection current.

iii. The nonlinear phase shift increase with decrease injection current.

The nonlinear phase-shift of SOA per unit length can be expressed as shown in equation 11. The parameter (α_2) has a negative sign therefore the contribution of the second term to the phase-shift is always positive. Hence, at zero current the equation predict the highest phase-shifts, while for

higher currents the phase-shift decreases due to the smaller contribution of the first term. If an ultrashort optical control pulse is fed into an SOA that is operated at zero injection current, it will generate carriers, not only directly by absorption but also by TPA. These latter carriers are hot, but will cool down on a sub-picosecond time scale and will already lead to an extra increase of the gain within the carrier–carrier scattering time (50–100 fs), all of which leads to a positive phase shift. On the other hand, if the injection current is increased to a value above transparency, a reservoir of carriers is available in the conduction and valence bands. As soon as the optical control pulse passes by, these carriers recombine due to stimulated emission followed by a recovery of the carrier number due to TPA and cooling. In this case, the negative gain induced contribution to the phase shift counteracts the positive instantaneous TPA induced contribution. For a specific injection current, the value of which depends on the control pulse energy, the net phase-shift vanishes. For this injection current, the phase-shift due to the stimulated emission is precisely compensated by the phase-shift due to TPA. If the injection current is increased further the net phase shift is dominated by the stimulated emission and saturates for high injection currents.

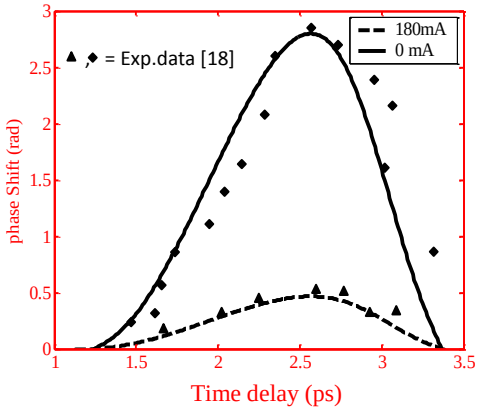

Figure 6 Nonlinear phase shifts as a function of the Control–probe delay time, for I =0 mA (solid line) and I = 180 mA (doted line). The control pulse energy is 3 pJ and the probe pulse energy is 0.3 pJ.

E.TPA effect on phase dynamics

Figure 7 shows the variation of phase shift with time delay when TPA is neglected (broken line) and assuming I=0mA. The solid line in the figure indicates the results when TPA is included in the calculation Figure 7 can be explain according to equation 11. In this equation, the first term (gain depletion and ultrafast recovery due to carrier cooling) is proportional to the injection current (I). For sufficiently small injection current, the nonlinear phase shift is positive but it is lower compared with the case when TPA is present. This decrease is due to the absence of the positive value of the nonlinear phase shift introduced by TPA, where TPA gives always positive phase shift. When the injection current (I) continues to increase and at certain current which depends on control energy the nonlinear phase shift due to gain depletion turns to negative due to depletion.

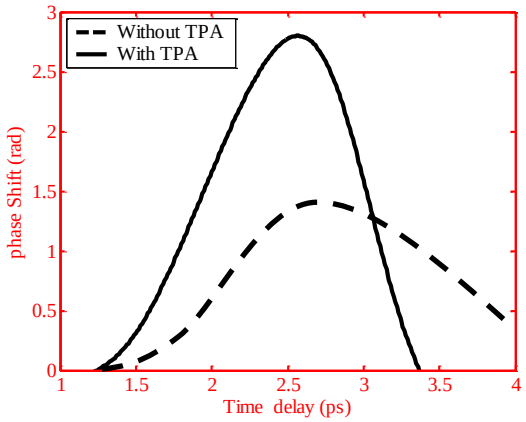

Figure 7 Effect of TPA on nonlinear phase shift, injection current I=0mA.

F. Effect of SOA length

Figure 8 shows the dependence of nonlinear phase shift $\Delta\Phi_{NL}$ on the length of active region. The solid and broken lines refers, respectively, to 10 GHz and 40GHz control repetition frequency. The optimum length, which makes $\Delta\Phi_{NL} = \pi$ is 0.75 (1.55) mm for 10 (40) GHz repetition frequencies. When the length of the SOA increase beyond 1.55mm, the nonlinear phase shift starters to decrease due to saturation effect in the SOA.

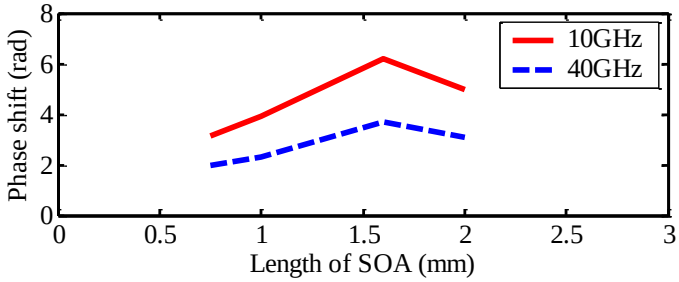

Figure 8 Nonlinear phase shift obtained versus SOA cavity length.

Figure 9a illustrates the dependence of nonlinear phase shift $\Delta\Phi_{NL}$ on control pulse energy at 10 GHz control repetition frequency and taking the length of SOA active region as an independent parameter. In these calculations, the values of L consider here are 0.75, 1 and 1.55 mm. The width and thickness of the active region are assumed to be constant at 2μm and 0.1 μm respectively. The calculation is repeated in Figure 9b for 40GHz control repetition
frequency. Investigating Figures 9a and 9b reveals that $\Delta\Phi_{NL}$ increases with cavity length for the range of L considered here. For example to achieve $\Delta\Phi_{NL} = \pi$ for 10(40)GHz, at control pulse energy of 3.4pJ, L=0.75(1.55) mm.

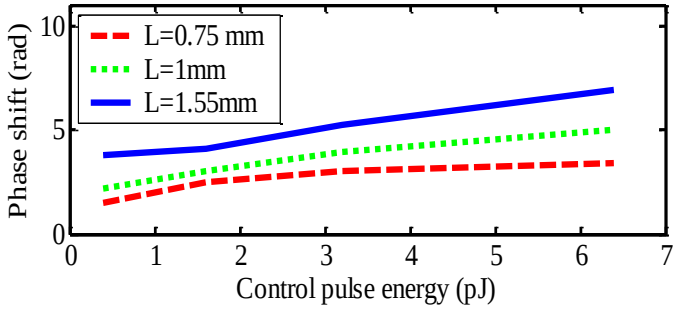

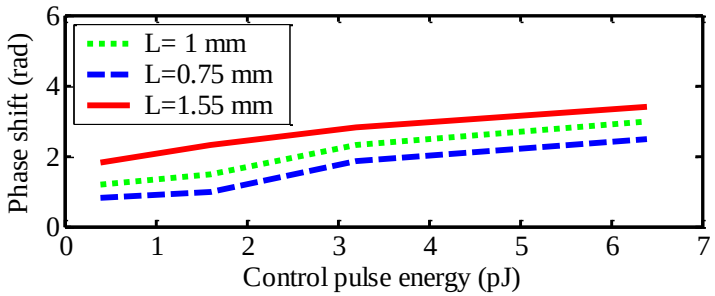

Figure 9 Nonlinear phase shift versus control pulse energy different SOA cavity length at zero SOA bias current for a) control repetition frequency 10GHz b) control repetition frequency 40GHz

IV Conclusion

The maximum phase shift in MQW SOAs increases with control pulse energy and decrease with driving current control pulse repetition rate. The important results the maximum nonlinear phase-shift induced in the SOA by 200 fs optical pulses phase-shift increases with decreasing injection current. This result is essentially different from those cases in which the nonlinear phase-shift is introduced by picosecond optical pulses, since in the latter cases the effect of TPA is irrelevant. The nonlinear phase-shift recovers in approximately 1.8 ps.The maximum nonlinear phase-shift in semiconductor optical amplifiers is obtained at zero injection current. This result might be relevant for researchers in the OTDM community since it suggests that it is beneficial to employ optically pumped passive waveguides for ultrafast optical time domain demultiplexing instead of active waveguides. The largest decrease in the TE gain takes place if the control pulse is also purely TE polarized and the smallest variation in the TE gain takes place if the control pulse is purely TM polarized. The nonlinear phase shift contains two contributions, one due to the phase shift introduced by the carrier depletion and the other due to the direct nonlinear phase shift introduced by TPA.The maximum phase shift, that could be reached is 3.1 rad in the 0.75 (1.6) mm long MQW-SOA at a control pulse rate 10 (40) GHz and control pulse energy 3.2 pJ.

References :

1. K. Kikuchi and K. Matsuura, "Transmission of 2-ps optical pulses at 1550 nm over 40-km standard fiber using midspan optical phase conjugation in semiconductor optical amplifiers," IEEE Photon. Technol. Lett., 10, pp. 1410–1412, 1998.

2. S. Diez, C. Schmidt, R. Ludwig, H. G. Weber, K. Obermann, S. Kindt, I. Koltchanov, and K. Petermann, "four-wave mixing in semiconductor optical amplifiers for frequency conversion and fast optical switching," IEEE Journal of Select Topics Quantum Electron., 3, pp. 1–15, 1997.

3.O.Wada " Femtosecond all-optical devices for ultrafast communication and signal processing" New Journal of Physics, 6 ,pp.183-185 , 2004.

4.H.J.S. Dorren, H. Ju, X. Yang, E. Tangdiongga "All-optical logic based on ultra-fast nonlinearities in a semiconductor optical amplifier " Cobra Research Institute, Eindhoven University of Technology.

5. J. A. Gruetzmacher M. A. Horn " Gain-switched, all-acousto-optic, femtosecond pulse amplifier" Review of scientific instrument , 74,pp.4961-4965, 2003.

6. A. M. Melo, V. Marembert," Design optimization of ultra-high bit-rate NOLM-based OTDM demultiplexers" IEEE, pp.905-906,2005.

7. S.A. Hamilton, B.S. Robinson, T.E. Murphy "100 Gb/s Optical Time-Division Multiplexed Networks" Light wave technology , 20,pp.2086-2090,2002.
8. J. Mørk and A. Mecozzi, "Theory of the ultrafast optical response of active semiconductor waveguides", J. Opt. Soc. Am. B., 13, pp. 1803-1816, 1996.
9. J. Mørk, S. Bischoff, T. W. Berg and M. L. Nielsen " Ultrafast optical signal processing in semiconductor optical devices" COM, Technical University of Denmark.
10. M. Connelly " Characterisation and modelling of SOA wavelength router" Optical Communications Research Group.
11. G.E. Sartoris " Modeling semiconductor optical devises " journal of modeling and simulation of microsystem,1 ,pp. 1-8,1999.
12. X. Yang, D. Lenstra, and H.J.S. Dorren " Phase-shift stabilization of 500 Gbit/s ultra-short optical pulses in a semiconductor optical amplifier by Manchester encoding" COBRA Research Institute, Eindhoven University of Technology,pp.302-305,2002.
13. M. Sheik-Bahae, E.W. Van Stryland " Ultrafast nonlinearities in semiconductor laser amplifier" Physical Review B, 50, pp.171-178, 1994.
14. J. Mork and J. Mark " Carrier Heating in InGaAsP Laser Amplifiers" IEEE Journal of selected topics in quantum electronics, 3, pp.1190-1205, 1994.
15. L. Occhi, Y. Ito " Intraband Gain Dynamics in Bulk Semiconductor Optical Amplifiers: Measurements and Simulations " IEEE journal of quantum electronic , 38, pp.54-59, 2002.
16. G. P. Agrawal and N. A. Olsson, "Self-Phase Modulation and Spectral Broadening of Optical Pulses in Semiconductor Laser Amplifiers",Journalof Quantum Electronics., 25, pp. 2297 - 2306, 1989.
17 X.Yanga, D. Lenstra , A.K. Mishra "Propagation of ultrashort optical pulses in a semiconductor optical amplifier: simulation and experiments' Cobra Research Institute, Eindhoven University of Technology.
18. X. Yang, A.K. Mishra, D. Lenstra "Sub-picosecond all-optical switch using amulti-quantum-well semiconductor optical amplifier" Optics Communications 236 ,pp.329–334, 2004.